Check for updates

Tedeschi Sara K (Orcid ID: 0000-0001-9475-1363)
Becce Fabio (Orcid ID: 0000-0001-8444-8504)
Pascart Tristan (Orcid ID: 0000-0002-8395-826X)
Budzik Jean-François (Orcid ID: 0000-0002-6009-5705)
Dalbeth Nicola (Orcid ID: 0000-0003-4632-4476)
Filippou Georgios (Orcid ID: 0000-0002-1647-2083)
Choi Hyon (Orcid ID: 0000-0002-2862-0442)

Accepted Article

Imaging features of calcium pyrophosphate deposition (CPPD) disease: consensus definitions from an international multidisciplinary working group

Sara K. Tedeschi, MD, MPH,[1] Fabio Becce, MD,[2] Tristan Pascart, MD, PhD,[3] Ali Guermazi, MD, PhD,[4] Jean-François Budzik, MD, PhD,[5] Nicola Dalbeth, MD,[6] Georgios Filippou, MD, PhD,[7] Annamaria Iagnocco, MD,[8] Minna J. Kohler, MD,[9] Jean-Denis Laredo, MD,[10] Stacy E. Smith, MD,[11] F. Joseph Simeone, MD,[12] Janeth Yinh, MD,[9] Hyon Choi, MD, PhD,[9] Abhishek Abhishek, MBBS, MD, FRCP, PhD[13]

1. Division of Rheumatology, Inflammation and Immunity, Brigham and Women's Hospital and Harvard Medical School, Boston, United States
2. Department of Diagnostic and Interventional Radiology, Lausanne University Hospital and University of Lausanne, Lausanne, Switzerland
3. Department of Rheumatology, Lille Catholic University, Lille, France
4. Department of Radiology, Boston VA Healthcare System, Boston University School of Medicine, Boston, USA
5. Department of Diagnostic and Interventional Radiology, Lille Catholic Hospitals, Lille, France
6. Department of Medicine, University of Auckland, Auckland, New Zealand
7. Division of Rheumatology, Luigi Sacco University Hospital, Milan, Italy

This article has been accepted for publication and undergone full peer review but has not been through the copyediting, typesetting, pagination and proofreading process which may lead to differences between this version and the Version of Record. Please cite this article as doi: 10.1002/acr.24898

This article is protected by copyright. All rights reserved.

Accepted Article

8. Academic Rheumatology Centre, Dipartimento Scienze Cliniche e Biologiche, Università degli Studi di Torino, Turin, Italy
9. Division of Rheumatology, Allergy, and Immunology, Massachusetts General Hospital and Harvard Medical School, Boston, United States
10. Department of Orthopedic Surgery, Hôpital Lariboisière, Assistance Publique des Hôpitaux de Paris, UMR CNRS 7052, Université de Paris, Paris, France
11. Division of Musculoskeletal Imaging and Intervention, Department of Radiology, Brigham and Women's Hospital and Harvard Medical School, Boston, United States
12. Department of Radiology, Massachusetts General Hospital and Harvard Medical School, Boston, United States
13. Department of Academic Rheumatology, University of Nottingham, Nottingham, United Kingdom

Corresponding author

Sara K. Tedeschi, MD, MPH

Brigham and Women's Hospital

Division of Rheumatology, Inflammation and Immunity

60 Fenwood Road, Suite 6016

Boston, MA 02115 United States

stedeschi1@bwh.harvard.edu

tel: +1 617 732 5325

fax: +1 617 732 5766

Accepted Article

Funding: The project was supported by joint funding from the American College of Rheumatology and European League Against Rheumatism. Dr. Tedeschi receives support from the National Institutes of Health (K23 AR075070, L30 AR070514).

Word count: 3338

Keywords: CPPD, calcium pyrophosphate deposition, imaging

Disclosures

- Sara Tedeschi: Consulting fees from NGM Biopharmaceuticals (<10K); Co-Chair, OMERACT CPPD Working Group
- Fabio Becce: Consulting fees from Horizon Therapeutics (<10K); research agreement for dual-energy CT with Siemens Healthineers
- Tristan Pascart: Consulting fees from Novartis (<10K) and Research grants from Horizon Pharmaceuticals
- Ali Guermazi: Shareholder BICL, LLC, Consulting fees from Pfizer, MerckSerono, TissueGene (>10K), AstraZeneca, Regeneron, and Novartis (<10K)
- Nicola Dalbeth: Consulting fees from AstraZeneca, Dyve, Selecta, Horizon, Arthrosi, PK Med, JW Pharmaceutical Corporation, and Cello Health (all <10K). Speaker fees from Abbvie and Janssen (all <10K); Co-Chair, OMERACT CPPD Working Group
- Annamaria Iagnocco: Consulting fees and speaker fees from: Abbvie, MSD, Alfasigma, Celltrion, BMS, Celgene, Eli-Lilly, Sanofi Genzyme, Pfizer, Galapagos, Gilead, Novartis
- Minna J. Kohler: Consultant fees from Novartis, speaker fees from Lilly

- Jean-Denis Laredo: Consulting and lectures fees for Pfizer, Lilly, Novartis, UCB, Genevrier, Mylan. Research grants from Siemens and Thales.
- Hyon Choi: payments from ACR/EULAR for the CPPD Classification Criteria working group projects made to his institution
- Abhishek Abhishek: Consulting fees from NGM Biopharmaceuticals (<10K); Co-Chair, OMERACT CPPD Working Group; payments from ACR/EULAR for the CPPD Classification Criteria working group projects made to his institution
- Budzik, Filippou, Smith, Simeone, Yinh: No conflicts to declare.

Accepted Article

Accepted Article

ABSTRACT

Objectives: To develop definitions for imaging features being considered as potential classification criteria for calcium pyrophosphate deposition (CPPD) disease, additional to clinical and laboratory criteria, and to compile example images of CPPD on different imaging modalities.

Methods: The ACR/EULAR CPPD classification criteria Imaging Advisory Group (IAG) and Steering Committee drafted definitions of imaging features that are characteristic of CPPD on conventional radiography (CR), conventional computed tomography (CT), dual-energy CT (DECT), and magnetic resonance imaging (MRI). An anonymous expert survey was undertaken by a 35-member Combined Expert Committee including all IAG members. The IAG and five external musculoskeletal radiologists with expertise in CPPD convened virtually to further refine item definitions, and voted on example images illustrating CR, CT, and DECT item definitions with ≥90% agreement required to deem them acceptable.

Results: The Combined Expert Committee survey indicated consensus on all CR definitions. The IAG and external radiologists reached consensus on CT and DECT item definitions, which specify that calcium pyrophosphate deposits appear less dense than cortical bone. The group developed an MRI definition and acknowledged limitations of this modality for CPPD. Ten example images for CPPD were voted acceptable (4 CR, 4 CT, 2 DECT), and three example images of basic calcium phosphate deposition were voted acceptable to serve as contrast against imaging features of CPPD.

Conclusion: An international group of rheumatologists and musculoskeletal radiologists defined imaging features characteristic of CPPD on CR, CT, and DECT, and assembled a set of example images as a reference for future clinical research studies.

Accepted Article

Significance and Innovation

- An international group of rheumatologists and musculoskeletal radiologists with expertise in CPPD developed consensus-based definitions of imaging features characteristic of CPPD on conventional radiography, conventional CT, and dual-energy CT.
- These definitions signal key elements that are considered specific to CPPD on CR, CT, and DECT, and can be applied in research studies and clinical practice.
- Example images of CPPD provide a useful reference for clinical practice and for future application of CPPD classification criteria once validated.

Accepted Article

INTRODUCTION

Calcium pyrophosphate deposition (CPPD) disease affects tens of millions of adults worldwide.[1-5] Patients with this common crystalline arthritis can experience one or more of its manifestations, namely acute calcium pyrophosphate (CPP) crystal arthritis, chronic CPP crystal inflammatory arthritis, and CPPD with osteoarthritis (OA) over time or simultaneously. Classification criteria for CPPD will allow investigators to identify patients with any of these manifestations for clinical research studies.[6,7] The American College of Rheumatology (ACR) and European Alliance of Associations for Rheumatology (EULAR) are jointly sponsoring development of CPPD classification criteria using data- and expert-driven methods previously used for other rheumatic diseases.[8-13]

The ACR/EULAR CPPD Classification Criteria working group recently reported the results of item generation and item reduction phases, the first two of a four-phase process.[14] These processes resulted in a large number of imaging candidate items, spanning a variety of modalities including conventional radiography (CR), ultrasound (US), conventional computed tomography (CT), dual-energy CT (DECT), and magnetic resonance imaging (MRI). The imaging items sort into two main groups: (1) osteoarthritis of specific joints and (2) calcification characteristic of CPPD in target structures including fibrocartilage or hyaline cartilage, synovial membrane or joint capsule, and tendon.

CR is the first-line imaging modality and a widely-used technique for identifying calcification, though a standard CR definition of CPPD has yet to be developed. EULAR developed

Accepted Article

recommendations for CPPD terminology and diagnosis in 2011, and recognized radiographic cartilage calcification as an important feature but did not provide a formal definition or description of this finding on CR.[2] US definitions for CPPD have been developed and validated by the OMERACT CPPD US Subtask Force.[15-17] Descriptions of findings characteristic of CPPD on emerging imaging modalities such as DECT and MRI are needed. Additionally, specifying features that differentiate CPP crystal deposits from other calcium-containing deposits, primarily basic calcium phosphate (BCP) crystal deposits, is also of paramount importance.

This manuscript reports on the development of CPPD imaging item definitions by an international group of rheumatologists and musculoskeletal radiologists. A set of example images of CPPD was curated to serve as a reference for future use.

METHODS

Development of imaging definitions

The CPPD classification criteria working group includes a 35-member Combined Expert Committee subdivided into Clinical, Imaging, and Laboratory Advisory Groups; a subset comprises the Steering Committee. Definitions of imaging findings characteristic of CPPD were developed to ensure consistency in future data collection across international medical centers; this process occurred in parallel with item generation and item reduction for CPPD classification criteria development.[14] The Imaging Advisory Group and Steering Committee agreed to adopt previously published OMERACT US definitions for CPPD in cartilage and tendon, and additionally drafted US definitions for CPPD in synovial membrane and joint capsule as these

Accepted Article

were candidate items (see **Supplementary Table 1**).[15] Imaging item definitions for CR, CT, DECT, and MRI were initially drafted by the Imaging Advisory Group content-area expert (FB, musculoskeletal radiologist), Steering Committee liaison (TP, rheumatologist), and one co-PI of the classification criteria working group (AA, rheumatologist). Imaging Advisory Group members (FB, TP, ND, GF, AI, MK, JY) reviewed draft definitions for face validity. Draft definitions were emailed to the Combined Expert Committee with an invitation to complete an online survey using Microsoft Office Forms regarding acceptability of each, with opportunity to provide comments. The Imaging Advisory Group and Steering Committee reviewed survey responses and collated free-text comments.

Steering Committee members nominated five external musculoskeletal radiologists (AG, JFB, JDL, SS, JS) with expertise in CPPD imaging to provide input on definitions for which Combined Expert Committee members raised questions on the online survey, namely for CT, DECT, and MRI. Imaging Advisory Group members and external radiologists held a videoconference to discuss and refine item definitions. Meeting minutes were circulated by email, edited by participants, and re-circulated iteratively until there were no objections to the proposed definitions. Imaging features of crowned dens syndrome were drafted and iteratively discussed by email with clinical and imaging experts. Definitions were then considered to be final.

Assembling example images of CPPD

Imaging Advisory Group members and the external musculoskeletal radiologists curated a set of example images illustrating the features described in the item definitions for future reference.

Accepted Article

De-identified CR, CT, and DECT images were uploaded to Google Forms labeled with the definition that each image was intended to illustrate. Imaging Advisory Group members (n=7), the external musculoskeletal radiologists (n=5), and one co-PI of the classification criteria working group were invited to vote whether each image was acceptable and provide comments. At least 90% agreement on an image being acceptable was required for retention. Additional images were submitted by Steering Committee members and external radiologists for a second round of voting when zero or only one image for a modality or characteristic joint was acceptable in the first round of voting. US images were not solicited as OMERACT has published example images.[15,17]

This work did not involve human subjects research and as such Institutional Review Board approval was not obtained.

RESULTS

Of the 53 items remaining after the item reduction phase, 23 (43%) were imaging items. These included imaging evidence of calcification consistent with CPPD in the knee, wrist, and one additional joint, and evidence of OA at particular joints in the hand and wrist. **Supplementary Table 1** provides a complete list of candidate imaging items.

Twenty members of the Combined Expert Committee (57%) participated in the item definition survey. Free text comments revealed questions about item definitions referring to BCP as a counterexample to CPPD and regarding technical parameters for DECT.

Accepted Article

Table 1 provides preliminary definitions discussed by Imaging Advisory Group members and external musculoskeletal radiologists during the videoconference, and final item definitions.

Conventional radiography

CR definitions of CPPD were all deemed acceptable by the Combined Expert Committee on the survey and are presented in **Table 1**.

Ultrasound

New US definitions of CPPD in synovial membrane and joint capsule were based upon previously validated definitions for US findings of CPPD in fibro- or hyaline cartilage developed by the OMERACT CPPD US Subtask Force. Key features include hyperechoic deposits of variable shape and size located within the structure of interest (synovial membrane or joint capsule) that do not create posterior shadowing.

Conventional CT

The first aspect discussed was the location and morphology of calcifications. While intra-articular location of calcifications is more characteristic of CPP than BCP deposits, BCP can be present within the joint space (e.g. Milwaukee shoulder syndrome) and CPP can be found in peri-articular structures (e.g. cruciate ligament of the atlas), so location was not felt to be a definitive distinguishing feature.[18] Morphology of calcifications from CPP versus BCP was discussed at length. CPP deposits are typically fine linear or punctate, but can be denser in long-standing CPPD. By contrast, BCP deposits are generally larger, homogeneous and well-defined ("cloudlike"), and denser in the formative and resting phases, but become fluffy, ill-defined, and

Accepted Article

less dense during episodes of crystal resorption as previously described by Uhthoff.[19] Concerns were raised about distinguishing between punctate CPP deposits and cloudlike BCP deposits. The group considered specifying a threshold size for CPP deposits in greatest dimension, but a threshold would require testing and validation outside the scope of the current work. Consensus was reached to simply state "linear or punctate" and present example images to illustrate this definition.

The second aspect discussed was determining a density specific for CPPD. It was noted that because windowing can be adjusted to make an image appear more or less contrasted, a reference point for density was needed because CPP deposits should typically be less dense than the central portion of BCP and cortical bone.[20] BCP was removed as the reference for density due to concerns about distinguishing CPP from BCP on CT based on density alone. Although indicative to some extent, absolute number of Hounsfield units (HU) was removed from the definition for several reasons, including the dependence of CT numbers of calcifications on the CT acquisition protocol, in particular the tube potential (in kV). The group reached consensus that the proposed threshold of <300 HU was uncertain, as both CPP and BCP can have HU between 300-450 HU.[20-22] A threshold of <200 HU was considered to differentiate between CPP and BCP, but would exclude the vast majority of CPP deposits with higher HU. The group reached consensus to use cortical bone as a reference, since CPP is less dense than cortical bone and cortical bone will be visible on images. As a separate point, it was noted that HU can be difficult to assess if CT images are viewed without using a PACS workstation.

Dual-energy CT

Accepted Article

DECT scans should demonstrate dual-energy ratio (DER), dual-energy index (DEI) or effective atomic number (Z_{eff}) values characteristic of CPP deposits to ensure specificity. Several concerns were raised about including Z_{eff} in item definitions, especially because the Z_{eff} varies with calcium crystal concentration. Limited data on Z_{eff} for CPP deposits suggest a range of approximately 8.5-10, which overlaps with the lower range of the Z_{eff} for BCP at crystal concentrations encountered in vivo.[21,22] The peripheral, less concentrated/"dense" portion of BCP deposits can reach Z_{eff} values as low as 9.3.[20] Consensus was reached that this preliminary threshold, which has been determined for only a few DECT systems and acquisition protocols to date, needs to be refined with more data using a range of DECT systems and acquisition protocols, and would be omitted. Additionally, calculating Z_{eff} may be time-intensive depending on the post-processing software used, raising concerns about feasibility.

DER and DEI are two similar representations of the same measure, with the difference being that DER is simpler and refers only to the ratio of low kV x-ray attenuation divided by high kV attenuation. Consensus was reached to include DEI in the definition along with a formula for calculating DEI from high and low kV CT images on a PACS workstation (see **Table 1**). The reference range for DEI of CPP deposits was based upon prior studies showing that the DEI in meniscal chondrocalcinosis of people with CPPD ranged from 0.016-0.039 versus 0.041 ± 0.005 for low-concentration BCP deposits in patients with calcific tendinitis of the shoulder.[20,22] The optimal cut-off DEI of 0.036 for CPPD was determined to minimize the risk of overlapping with the DEI most suggestive of BCP.[20] Switching from DEI to DER would provide similar results with similar caveats, except for adapted reference ranges. It is important to bear in mind that the reference ranges for DER and DEI must take into account both the DECT systems and

Accepted Article

acquisition protocols (i.e. x-ray beam spectral separation) used, in addition to relying on crystal calibration phantoms, as recently demonstrated in a phantom study.[23] Absolute number of HU was removed and density of cortical bone was added as a reference point, as for conventional CT.

MRI

Evidence of CPPD on ultrashort echo time (UTE), susceptibility-weighted imaging (SWI), or 3-dimensional (3D) dual-echo steady-state (DESS) MRI sequences was discussed.[24-26] There was low enthusiasm overall for this modality due to lack of specificity data in CPPD compared to BCP deposits, as MRI is not intended to characterize the types of calcium crystal deposits but only to detect and quantify them. The general sentiment was that MRI is less specific for CPPD than CT or DECT. Long acquisition time and advanced data post-processing also make MRI a less feasible method for evaluating CPPD, particularly in patients with acute CPP crystal arthritis. The consensus definition for evidence of CPPD on MRI was "linear or punctate regions of low signal intensity located mainly in avascular white and red-white zones of menisci, and within hyaline cartilage surfaces, visible on dedicated specific (e.g. UTE or SWI) MR sequences." While MRI can provide additional information about presence of radiologic hand OA, the group agreed that MRI was unlikely to contribute additional information specific to CPP deposits compared to BCP deposits above and beyond the other imaging modalities.

Crowned dens syndrome imaging definition

Imaging features of crowned dens syndrome include conventional CT with calcific deposits, typically linear and less dense than cortical bone, in the transverse retro-odontoid ligament

(transverse ligament of the atlas), often with an appearance of two parallel lines in axial views. Calcifications at the atlanto-axial joint, alar ligament, and/or in pannus adjacent to the tip of the dens are also characteristic. If DECT is performed, the DEI of the calcification should be between 0.016-0.036. It should be noted that these imaging findings taken alone do not define crowned dens syndrome; characteristic clinical features must also be present.

Radiographic OA at hand/wrist

The group adopted definitions for presence of radiographic OA at certain hand joints that associate with CPPD[27-29] and may potentially discriminate between cases with CPPD and mimickers.[14] We utilized widely used and established atlases of hand OA, and defined radiographic OA at the radiocarpal joint or the 2nd or 3rd metacarpophalangeal joints as Kellgren-Lawrence grade 2 or more; scapho-trapezium joint OA is defined by presence of either joint space narrowing and/or osteophytes as per the 2007 Osteoarthritis Research Society International (OARSI) atlas.[30,31] We refer readers to representative images published in these atlases.

Example images of CPPD

Ten of 13 invited participants voted on five CR, five CT, and three DECT images in the first voting round. Eight of 13 images (62%) were deemed acceptable by ≥90% of participants. Reasons for voting images unacceptable included nummular appearance of calcifications rendering inability to discriminate between BCP and CPP (CR); tendon calcification small and difficult to see (CT); lesion not clearly marked (DECT); unusual multiplanar reconstruction planes (DECT); images blurred with insufficient spatial resolution. Participants suggested

Accepted Article

Accepted Article

including images of crowned dens syndrome and reference images of BCP, as the contrast between location and appearance of CPP and BCP deposits is paramount.

Twelve of 13 invited participants responded in a second round of voting. This included five images of CPPD (four CT, one DECT) and six images of BCP (five CR, one CT paired with DECT). Five of 11 images (45%) were deemed acceptable. Comments about unacceptable images included: diffuse hyperdense joint effusion on CT not typical of CPPD and could represent hemarthrosis; tendon calcification appears indistinguishable from BCP calcific tendinitis and could be post-traumatic. Comments on unacceptable images for BCP noted linear appearance that could be confused for CPPD or represent ligamentous ossification (Pellegrini-Stieda lesion); location of calcification in synovium or bursa that could be either CPP or BCP deposition; too faint calcification in the shoulder that is not classic for BCP deposition; densities in the tibiofemoral compartment might represent osteochondromas from advanced OA or BCP deposition.

The example images of CPPD on CR (**Figures 1-2**), CT (**Figures 3-4** and **Supplementary Figure 1**), and DECT (**Figure 5**), and example images of BCP (**Supplementary Figure 2**) are presented herein.

DISCUSSION

Using a consensus-based process, an international group of rheumatologists and musculoskeletal radiologists with expertise in CPPD developed imaging definitions of CPPD for use in research studies and clinical practice. These definitions signal key findings that are considered specific to

Accepted Article

CPPD on CR, CT, and DECT. We compiled a set of example images vetted by experts in CPPD imaging for future reference. These definitions and images complement the OMERACT CPPD US definitions.[15-17]

At the conclusion of the item reduction phase of CPPD classification criteria development, nearly half of the candidate items were imaging findings relevant to CPPD.[14] Most pertain to characteristic calcifications, while others indicate OA at joints that are classically involved in CPPD. In the next phase of CPPD classification criteria development, related items will be clustered into domains, with hierarchical organization of items within domains. Items that are highly correlated may be further collapsed into one, and items may be eliminated if they do not discriminate between CPPD disease and mimicking conditions when tested in a development cohort based on de-identified patient cases.

CR specificity for CPPD is generally high (pooled specificity 96%) but variable across studies, while sensitivity is only moderate (pooled sensitivity 60%) in part due to its two-dimensional properties.[32,33] Standardized definitions for CPPD on CR have not previously been developed, and differences in definitions across studies might underlie some of the variability in the reported sensitivity and specificity.

The OMERACT CPPD US Subtask Force previously defined US features at sites commonly involved in CPPD that can be evaluated by US: fibrocartilage, hyaline cartilage, tendon, and synovial fluid.[15] A systematic literature review did not identify studies evaluating US performance for identifying CPPD in the synovial membrane or joint capsule, and OMERACT

Accepted Article

CPPD US Subtask Force did not develop definitions for these sites.[34] We developed definitions of CPPD in synovial membrane and joint capsule (see **Table 1**) as experts involved in developing CPPD classification criteria considered them potential discriminators between CPPD and other forms of arthritis. By contrast, US visualization of CPP deposits in synovial fluid was considered unlikely to distinguish CPPD from other forms of arthritis and was eliminated. US demonstrates good sensitivity (pooled sensitivity 81 to 88%) at the sites most frequently involved in CPPD, though reports of specificity for CPPD range from 59% to 92%.[16,33-36] While US offers high spatial resolution compared to other available imaging techniques, limitations in accuracy stem from its inability to definitively distinguish BCP from CPP deposits.[37]

Data on DECT performance in CPPD are currently limited, with two initial reports in small patient populations indicating good sensitivity (78% to 100%) and high specificity (94%).[38,39] DECT item definitions were refined to include a reference range for the DEI characteristic of CPP deposits, while minimizing overlap with the DEI of BCP. Future work to define reference ranges for DEI and DER characteristic of CPP on different DECT scanners will maximize reproducibility of results across medical centers. Recent data suggest that DECT may not add value to conventional CT in terms of sensitivity for detecting CPP deposits, including in anatomic structures where chondrocalcinosis is not visible macroscopically.[21] However, this technique has the potential to improve CT specificity by characterizing different types of calcifications. Among DECT attenuation parameters, Z_{eff} and particularly DEI or DER can help discriminate between CPP deposits and carbonate apatites, including BCP deposits, owing to a combination of higher density (both mass and electron) and Z_{eff} for BCP in vivo.[20,22,40] While Z_{eff} value is mainly related to photoelectric absorption, DEI or DER combines information from both

Accepted Article

photoelectric absorption and Compton scattering (which informs about mass and electron density).[41] Given that DECT adds value due to its spatial resolution properties, a cut-off DEI value of 0.036—corresponding to the lower bound of the reference range for low-concentration BCP deposits—was selected to limit the misclassification of low-concentration BCP deposits as false-positive CPP deposits.

Specific MRI sequences, such as UTE, SWI or DESS, were among the candidate items retained after item reduction, but in subsequent discussions were felt to be on the future research agenda for CPPD and not ready for routine clinical use nor for inclusion in CPPD classification criteria.[24-26,42] Recently, UTE and SWI MRI have shown promise for the identification and quantification of calcium crystal deposition in and around joints as well as other anatomical sites.[24,25,43,44]

Example images of CPPD presented herein will serve as a reference once the final classification criteria have been validated. These are not a comprehensive atlas of all possible imaging manifestations of CPPD, which was outside the scope of the current project. Rather, they provide visual examples illustrating the item definitions. Readers may find the BCP images useful as a counterpoint regarding the typical location, shape, size, and density of articular and peri-articular calcifications.

The limitations of this work include relying on an expert-based rather than data-driven process to develop item definitions. However, the definitions have face validity as they were developed by rheumatologists and musculoskeletal radiologists with expertise in clinical care of people with

Accepted Article

CPPD disease and CPPD research. Definitions of CR, CT, and DECT findings characteristic of CPPD, and US definitions at the synovial membrane and joint capsule, will need to be validated in independent cohorts.

CONCLUSION

We developed CPPD imaging item definitions for CR, CT, and DECT that will be used in subsequent phases of CPPD classification criteria development. Example images provide a guide for clinical practice and future application of the final validated CPPD classification criteria.

Contributorship: Drs. Tedeschi, Becce, Pascart, Dalbeth, Filippou, Iagnocco, Kohler, Yinh, Choi, and Abhishek conceived and planned the study. All authors participated in conducting the study. Drs. Tedeschi and Abhishek were responsible for data analysis and drafting the manuscript. Dr. Guermazi assembled the final figures. All authors provided constructive feedback on the manuscript and approved the final version.

Acknowledgements: The authors would like to thank the members of the ACR/EULAR CPPD Classification Criteria Combined Expert Committee for providing feedback on the draft definitions. We would also like to thank Prof Thomas Bardin for his expert input in developing the definition of crowned dens syndrome.

REFERENCES

Accepted Article

1. Abhishek A, Neogi T, Choi H, Doherty M, Rosenthal AK, Terkeltaub R. Review: Unmet Needs and the Path Forward in Joint Disease Associated With Calcium Pyrophosphate Crystal Deposition. Arthritis Rheumatol 2018;70:1182-91.
2. Zhang W, Doherty M, Bardin T, et al. European League Against Rheumatism recommendations for calcium pyrophosphate deposition. Part I: terminology and diagnosis. Ann Rheum Dis 2011;70:563-70.
3. Ramonda R, Musacchio E, Perissinotto E, et al. Prevalence of chondrocalcinosis in Italian subjects from northeastern Italy. The ProVA Study. Clin Exp Rheumatol 2009;27:981-84.
4. Maravic M, Ea HK. Hospital burden of gout, pseudogout and other crystal arthropathies in France. Joint Bone Spine 2015;82:326-9.
5. Felson DT, Anderson JJ, Naimark A, Kannel W, Meenan RF. The prevalence of chondrocalcinosis in the elderly and its association with knee osteoarthritis: the Framingham Study. J Rheumatol 1989;16:1241-5.
6. Aggarwal R, Ringold S, Khanna D, et al. Distinctions between diagnostic and classification criteria? Arthritis Care Res (Hoboken) 2015;67:891-7.
7. Singh JA, Solomon DH, Dougados M, et al. Development of classification and response criteria for rheumatic diseases. Arthritis Rheum 2006;55:348-52.
8. Neogi T, Jansen TL, Dalbeth N, et al. 2015 Gout Classification Criteria: an American College of Rheumatology/European League Against Rheumatism collaborative initiative. Arthritis Rheumatol 2015;67:2557-68.
9. Aletaha D, Neogi T, Silman AJ, et al. 2010 Rheumatoid arthritis classification criteria: an American College of Rheumatology/European League Against Rheumatism collaborative initiative. Arthritis Rheum 2010;62:2569-81.
10. Aringer M, Costenbader K, Daikh D, et al. 2019 European League Against Rheumatism/American College of Rheumatology classification criteria for systemic lupus erythematosus. Ann Rheum Dis 2019;78:1151-9.
11. van den Hoogen F, Khanna D, Fransen J, et al. 2013 classification criteria for systemic sclerosis: an American college of rheumatology/European league against rheumatism collaborative initiative. Ann Rheum Dis 2013;72:1747-55.
12. Fransen J, Johnson SR, van den Hoogen F, et al. Items for developing revised classification criteria in systemic sclerosis: Results of a consensus exercise. Arthritis Care Res (Hoboken) 2012;64:351-7.
13. Schmajuk G, Hoyer BF, Aringer M, et al. Multi-center delphi exercise reveals important key items for classifying systemic lupus erythematosus. Arthritis Care Res (Hoboken) 2018;70:1488-94.
14. Tedeschi SK, Pascart T, Latourte A, et al. Identifying potential classification criteria for calcium pyrophosphate deposition disease (CPPD): Item generation and item reduction. Arthritis Care Res 2021.
15. Filippou G, Scire CA, Damjanov N, et al. Definition and Reliability Assessment of Elementary Ultrasonographic Findings in Calcium Pyrophosphate Deposition Disease: A Study by the OMERACT Calcium Pyrophosphate Deposition Disease Ultrasound Subtask Force. J Rheumatol 2017;44:1744-9.
16. Filippou G, Scanu A, Adinolfi A, et al. Criterion validity of ultrasound in the identification of calcium pyrophosphate crystal deposits at the knee: an OMERACT ultrasound study. Ann Rheum Dis 2021;80:261-7.

Accepted Article

17. Filippou G, Scire CA, Adinolfi A, et al. Identification of calcium pyrophosphate deposition disease (CPPD) by ultrasound: reliability of the OMERACT definitions in an extended set of joints-an international multiobserver study by the OMERACT Calcium Pyrophosphate Deposition Disease Ultrasound Subtask Force. Ann Rheum Dis 2018;77:1194-9.
18. Freire V, Moser TP, Lepage-Saucier M. Radiological identification and analysis of soft tissue musculoskeletal calcifications. Insights Imaging 2018;9:477-92.
19. Uhthoff HK, Loehr JW. Calcific Tendinopathy of the Rotator Cuff: Pathogenesis, Diagnosis, and Management. J Am Acad Orthop Surg 1997;5:183-91.
20. Pascart T, Falgayrac G, Norberciak L, et al. Dual-energy computed-tomography-based discrimination between basic calcium phosphate and calcium pyrophosphate crystal deposition in vivo. Ther Adv Musculoskelet Dis 2020;12:1759720x20936060.
21. Budzik JF, Marzin C, Legrand J, Norberciak L, Becce F, Pascart T. Can Dual-Energy Computed Tomography Be Used to Identify Early Calcium Crystal Deposition in the Knees of Patients With Calcium Pyrophosphate Deposition? Arthritis Rheumatol 2021;73:687-92.
22. Pascart T, Norberciak L, Legrand J, Becce F, Budzik JF. Dual-energy computed tomography in calcium pyrophosphate deposition: initial clinical experience. Osteoarthritis Cartilage 2019;27:1309-14.
23. Døssing A, Müller FC, Becce F, Stamp L, Bliddal H, Boesen M. Dual-Energy Computed Tomography for Detection and Characterization of Monosodium Urate, Calcium Pyrophosphate, and Hydroxyapatite: A Phantom Study on Diagnostic Performance. Invest Radiol 2021.
24. Finkenstaedt T, Biswas R, Abeydeera NA, et al. Ultrashort Time to Echo Magnetic Resonance Evaluation of Calcium Pyrophosphate Crystal Deposition in Human Menisci. Invest Radiol 2019;54:349-55.
25. Nörenberg D, Ebersberger HU, Walter T, et al. Diagnosis of Calcific Tendonitis of the Rotator Cuff by Using Susceptibility-weighted MR Imaging. Radiology 2016;278:475-84.
26. Gersing AS, Schwaiger BJ, Heilmeier U, et al. Evaluation of Chondrocalcinosis and Associated Knee Joint Degeneration Using MR Imaging: Data from the Osteoarthritis Initiative. Eur Radiol 2017;27:2497-506.
27. Sanmarti R, Kanterewicz E, Pladevall M, Panella D, Tarradellas JB, Gomez JM. Analysis of the association between chondrocalcinosis and osteoarthritis: a community based study. Ann Rheum Dis 1996;55:30-3.
28. Peter A, Simmen BR, Bruhlmann P, Michel BA, Stucki G. Osteoarthritis of the scaphoidtrapezium joint: an early sign of calcium pyrophosphate dihydrate disease. Clin Rheumatol 2001;20:20-4.
29. Donich AS, Lektrakul N, Liu CC, Theodorou DJ, Kakitsubata Y, Resnick D. Calcium pyrophosphate dihydrate crystal deposition disease of the wrist: trapezioscaphoid joint abnormality. J Rheumatol 2000;27:2628-34.
30. Kellgren JH, Lawrence JS. Radiological assessment of osteo-arthrosis. Ann Rheum Dis 1957;16:494-502.
31. Altman RD, Gold GE. Atlas of individual radiographic features in osteoarthritis, revised. Osteoarthritis Cartilage 2007;15 Suppl A:A1-56.
32. McCarty DJ. Calcium pyrophosphate dihydrate crystal deposition disease: nomenclature and diagnostic criteria. Ann Intern Med 1977;87:241-2.
33. Cipolletta E, Filippou G, Scire CA, et al. The diagnostic value of conventional radiography and musculoskeletal ultrasonography in calcium pyrophosphate deposition disease: a systematic literature review and meta-analysis. Osteoarthritis Cartilage 2021.

Accepted Article

34. Filippou G, Adinolfi A, Iagnocco A, et al. Ultrasound in the diagnosis of calcium pyrophosphate dihydrate deposition disease. A systematic literature review and a meta-analysis. Osteoarthritis Cartilage 2016;24:973-81.
35. Lee KA, Lee SH, Kim HR. Diagnostic value of ultrasound in calcium pyrophosphate deposition disease of the knee joint. Osteoarthritis Cartilage 2019;27:781-7.
36. Gamon E, Combe B, Barnetche T, Mouterde G. Diagnostic value of ultrasound in calcium pyrophosphate deposition disease: a systematic review and meta-analysis. RMD Open 2015;1:e000118.
37. Bernabei I, Sayous Y, Raja AY, et al. Multi-energy photon-counting computed tomography versus other clinical imaging techniques for the identification of articular calcium crystal deposition. Rheumatology (Oxford) 2021.
38. Tanikawa H, Ogawa R, Okuma K, et al. Detection of calcium pyrophosphate dihydrate crystals in knee meniscus by dual-energy computed tomography. J Orthop Surg Res 2018;13:73.
39. Tedeschi SK, Solomon DH, Yoshida K, Vanni K, Suh DH, Smith SE. A prospective study of dual-energy CT scanning, US and X-ray in acute calcium pyrophosphate crystal arthritis. Rheumatology (Oxford) 2019.
40. Becce F, Viry A, Stamp LK, Pascart T, Budzik JF, Raja A. Winds of change in imaging of calcium crystal deposition diseases. Joint Bone Spine 2019;86:665-8.
41. Omoumi P, Becce F, Racine D, Ott JG, Andreisek G, Verdun FR. Dual-Energy CT: Basic Principles, Technical Approaches, and Applications in Musculoskeletal Imaging (Part 1). Semin Musculoskelet Radiol 2015;19:431-7.
42. Germann C, Galley J, Falkowski AL, et al. Ultra-high resolution 3D MRI for chondrocalcinosis detection in the knee-a prospective diagnostic accuracy study comparing 7-tesla and 3-tesla MRI with CT. Eur Radiol 2021.
43. Zehra U, Bow C, Cheung JPY, Pang H, Lu W, Samartzis D. The association of lumbar intervertebral disc calcification on plain radiographs with the UTE Disc Sign on MRI. Eur Spine J 2018;27:1049-57.
44. Du J, Peterson M, Kansal N, Bydder GM, Kahn A. Mineralization in calcified plaque is like that of cortical bone--further evidence from ultrashort echo time (UTE) magnetic resonance imaging of carotid plaque calcification and cortical bone. Med Phys 2013;40:102301.

FIGURE LEGENDS

Figure 1. Conventional radiographs of the hand and wrist characteristic of CPPD.

(a) Posteroanterior radiograph of the left hand shows linear and punctate calcifications of the triangular fibrocartilage complex (TFCC) (long arrow), radiocarpal joint (short arrow), and 2nd and 3rd MCP joint (arrowheads).

(b) Posteroanterior radiograph of the left wrist from a different patient demonstrates linear and punctate calcifications of the TFCC (long arrow), radiocarpal joint (short arrow), and inter-carpal joint hyaline cartilage (arrowhead).

Figure 2. Conventional radiographs of the knee and pelvis characteristic of CPPD.

(a) Anteroposterior radiograph of the right knee shows linear and punctate calcifications of the medial and lateral menisci (arrows) and femoral hyaline cartilage (arrowhead).

(b) Anteroposterior radiograph of the pelvis demonstrates linear calcifications of the fibrocartilage and hyaline cartilage of the pubic symphysis (white arrow), bilateral sacroiliac joints (yellow arrows), right and left hip hyaline cartilage (arrowheads), and left hip labral fibrocartilage (arrowheads). Large cloud-like calcification adjacent to the left ischial tuberosity may represent basic calcium phosphate deposition in the left ilio-psoas bursa or tendon; further imaging was not obtained.

Figure 3. Conventional unenhanced CT images of the knee and wrist characteristic of CPPD.

(a) Coronal reformatted CT images of bilateral knees show linear calcifications in the right knee hyaline cartilage (long arrows) and punctate calcifications in the left knee menisci (arrowheads).

(b) Coronal reformatted CT image of the right wrist from a different patient shows linear and punctate calcifications, less dense than cortical bone located within the TFCC (long arrow) and the scapholunate ligament (arrowhead).

Accepted Article

Accepted Article

Figure 4. Conventional unenhanced CT images of the cervical spine in a patient with crowned dens syndrome.

(a) Axial CT image at the level of the odontoid process shows linear calcifications involving the transverse and alar ligaments (arrows).

(b) Coronal reformatted CT image of the cervical spine demonstrates punctate calcifications and pannus adjacent to the tip of the dens (arrows).

Figure 5. Dual-energy CT images of the knee and wrist characteristic of CPPD.

(a) Coronal reformatted DECT image of the right knee shows linear calcifications of the menisci and hyaline cartilage. Color-code represents Z_{eff} values. The region of interest in the calcification (arrow) has a DEI of 0.028, within the expected range for CPP crystal deposition [22]. DECT was performed using a single-source CT system (Somatom Definition Edge; Siemens Healthineers, Erlangen, Germany). DECT measurements are made with syngo.via VB10B software, "Rho/Z" mode.

(b) DECT scan of the left wrist with axial, sagittal, and coronal reformats. Color-code represents Z_{eff} values. Punctuate calcifications (arrows) are visible in the extrinsic ligaments, on the palmar aspect of the scaphoid and lunate bones. Calcifications have a DEI of 0.027, within the expected range of CPP crystal deposition [22]. DECT was performed using a single-source CT system (Somatom Definition Edge; Siemens Healthineers, Erlangen, Germany). DECT measurements are made with syngo.via VB10B software, "Rho/Z" mode.

Accepted Article

Supplementary Figure 1. Conventional unenhanced CT images of the knee characteristic of CPPD.

(a) Sagittal reformatted CT image of the right knee shows linear and punctate calcifications, less dense than cortical bone located within the superficial hyaline cartilage of the lateral femoral condyle (long arrows).

(b) Sagittal reformatted CT image of the left knee from a different patient shows linear and punctate calcifications, less dense than cortical bone located within the deep hyaline cartilage of the lateral femoral condyle (long arrow) and the posterior cruciate ligament (arrowhead).

(c) Sagittal reformatted CT image of the left knee of the same patient as in (b) shows linear and punctate calcifications, less dense than cortical bone located within the deep hyaline cartilage of the medial femoral condyle (long arrows) and the anterior and posterior horns of the medial meniscus (arrowheads).

Supplementary Figure 2. Conventional radiographs with CT and DECT images characteristic of basic calcium phosphate (BCP) deposition.

(a) Anteroposterior conventional radiograph of the left shoulder shows dense amorphous cloudlike calcification with a well-defined contour within the subacromial space, in keeping with calcific tendinitis of the supraspinatus (arrows).

(b) Anteroposterior conventional radiograph of the right hip shows homogeneous dense and amorphous calcifications (arrows) projecting at the greater trochanter.

Conventional unenhanced axial CT image of the right knee (top image) shows a calcification as dense as cortical bone within the popliteal tendon, likely representing

BCP crystal deposition (arrow). Corresponding dual-energy axial CT image at the same level (bottom image) confirms BCP crystal deposition in the popliteal tendon (arrow). The calcification has a DEI of 0.079, higher than CPP crystal deposition and comparable to subchondral bone [22]. Color-code represents Z_{eff} values. Images from the post-treatment syngo.via VB10B software, "Rho/Z" mode, acquired using a single-source DECT system (Somatom Definition Edge; Siemens Healthineers, Erlangen, Germany).

Accepted Article

Accepted Article

Fig 1.tiff

Accepted Article

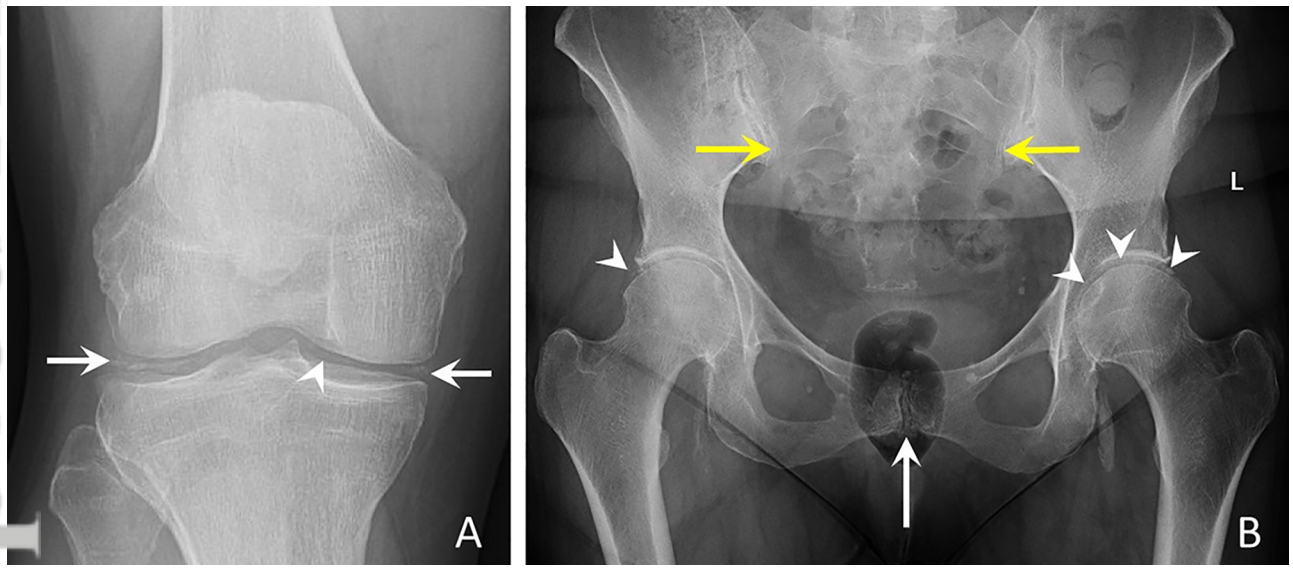

Fig_2(1).tiff

Accepted Article

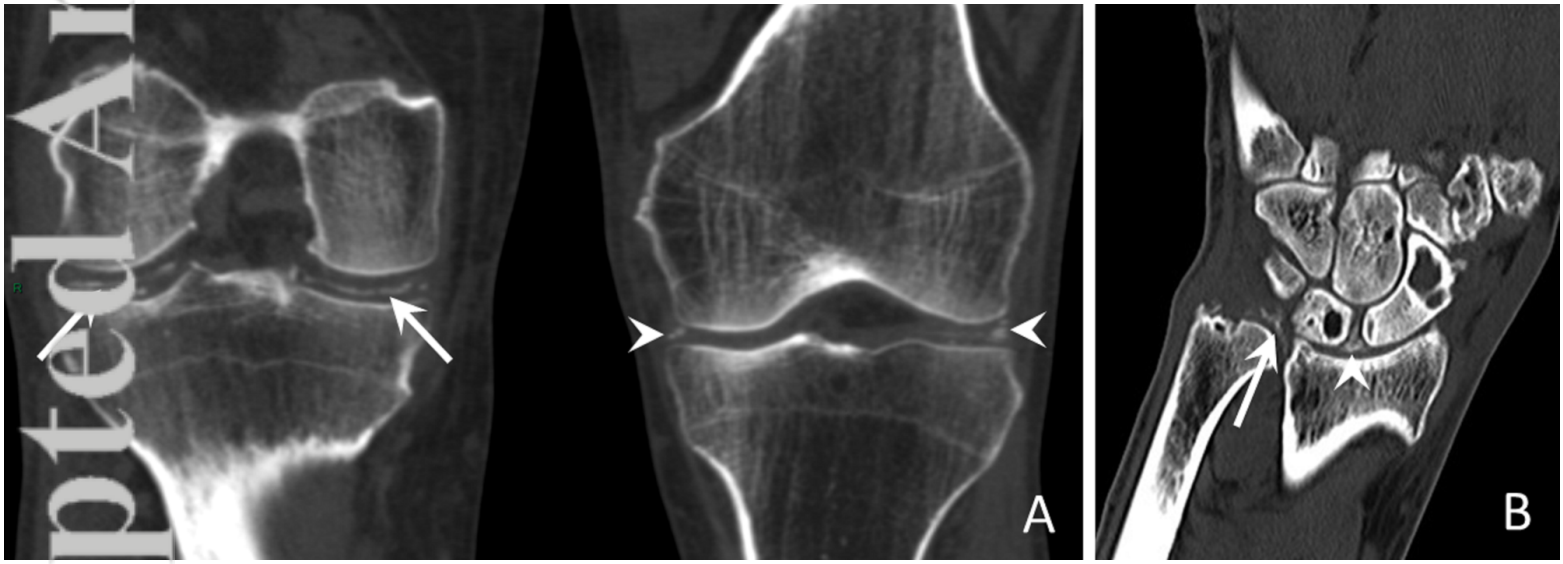

Figure 3.tif

Accepted Article

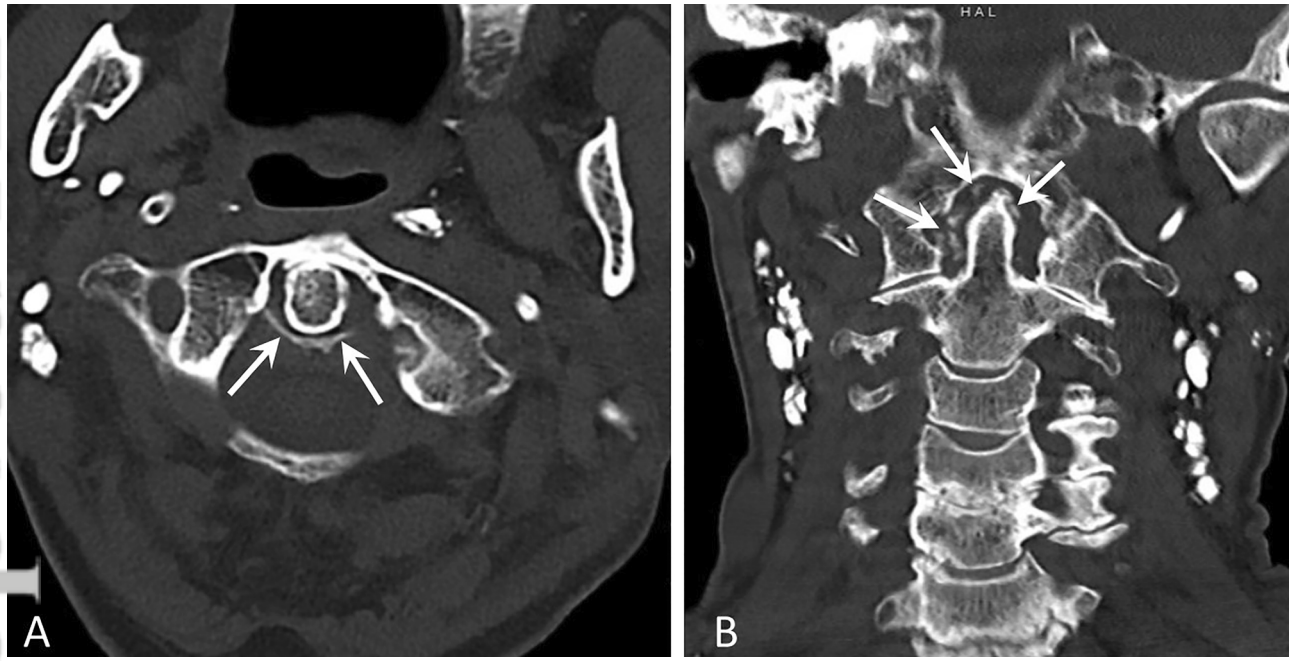

Fig 4.tiff

Accepted Article

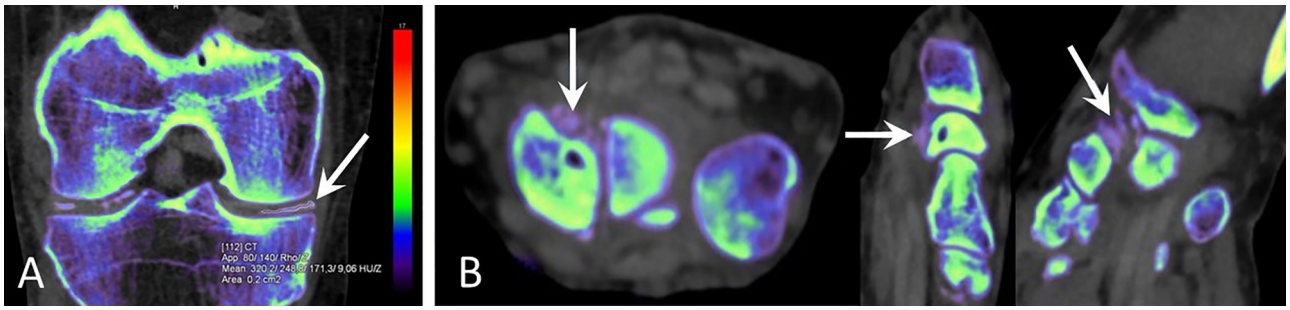

Fig 5.tiff

Accepted Article

Table 1. CPPD imaging item definitions

Item	Preliminary definition	Final definition
Conventional radiograph		
Calcification in fibro or hyaline cartilage on conventional radiograph	Linear or punctate opacities in the region of fibro or hyaline articular cartilage that are distinct from denser, nummular radio-opaque deposits due to BCP deposition	unchanged
Calcification of synovial membrane or joint capsule on conventional radiograph	Linear or punctate opacities in the region of synovial membrane or joint capsule that are distinct from denser, nummular radio-opaque deposits due to BCP deposition	unchanged
Calcification of tendon on conventional radiograph	Linear or punctate opacities within tendons or entheses that are distinct from denser, nummular radio-opaque deposits due to BCP deposition	unchanged
Conventional CT		
Calcification in fibro or hyaline cartilage on conventional CT	Generally well-defined, linear or punctate calcification, less dense (<300 HU) than BCP crystal deposition located mainly within the fibro or hyaline articular cartilage	Generally well-defined, linear or punctate calcification, less dense than cortical bone, located within the fibro or hyaline articular cartilage
Calcification of synovial membrane or joint capsule on conventional CT	Generally well-defined, linear or punctate calcification, less dense (<300 HU) than BCP crystal deposition located within the synovial membrane or joint capsule	Generally well-defined, linear or punctate calcification, less dense than cortical bone, located within the synovial membrane or joint capsule
Calcification of tendon on conventional CT	Generally well-defined, linear or punctate calcification, less dense	Generally well-defined, linear or punctate calcification, less dense

Accepted Article

	(<300 HU) than BCP crystal deposition located exclusively within tendons	than cortical bone, located within tendons
Dual-energy CT		
CPP crystal deposition in fibro or hyaline cartilage on DECT	Generally well-defined, linear or punctate, thinner, less dense (<300 HU) calcifications located mainly within the fibro or hyaline cartilage, with a dual-energy index (DEI) between 0.016-0.044 and Z_{eff} between 8.5-10	Generally well-defined, linear or punctate, thinner calcifications, less dense than cortical bone, located within the fibro or hyaline cartilage, with a dual-energy index (DEI) between 0.016-0.036*
CPP crystal deposition in synovial membrane on DECT	Generally well-defined, linear or punctate, thinner, less dense (<300 HU) calcifications located mainly within the synovial membrane or joint capsule, with a dual-energy index (DEI) between 0.016-0.044 and Z_{eff} between 8.5-10	Generally well-defined, linear or punctate, thinner calcifications, less dense than cortical bone, located within the synovial membrane or joint capsule, with a dual-energy index (DEI) between 0.016-0.036*
CPP crystal deposition in tendon on DECT	Generally well-defined, linear or punctate, thinner, less dense (<300 HU) calcifications located mainly within the tendons, with a dual-energy index (DEI) between 0.016-0.044 and Z_{eff} between 8.5-10	Generally well-defined, linear or punctate, thinner calcifications, less dense than cortical bone located within the tendons, with a dual-energy index (DEI) between 0.016-0.036*
Ultrasound^{+}		
Ultrasound evidence of CPP crystal deposition in fibro or hyaline cartilage^{+}	Hyperechoic deposits of variable shape and size, localized within the fibrocartilage or hyaline cartilage structure, that remain fixed or move along with the fibrocartilage/hyaline cartilage during dynamic assessment and do not create posterior shadowing^{+}	

Accepted Article

Ultrasound evidence of CPP crystal deposition in the synovial membrane, capsule, or tendon[+]	Synovial membrane: Hyperechoic deposits of variable shape and size, localized within the synovial membrane, that do not create posterior shadowing unless they reach large dimensions Joint capsule: Hyperechoic deposits of variable shape and size, localized within the capsule, that remain fixed and move along with the capsule during dynamic assessment and do not create posterior shadowing Tendon: Hyperechoic, linear structure(s) without posterior shadowing, localized within the tendon that remain fixed and move along with the tendon during dynamic assessment[+]	
Crowned dens syndrome**		
Imaging features of crowned dens syndrome**	Conventional CT with calcific deposits, typically linear and less dense than cortical bone, in the transverse retro-odontoid ligament (transverse ligament of the atlas), often with an appearance of two parallel lines in axial views. Calcifications at the atlanto-axial joint, alar ligament, and/or in pannus adjacent to the tip of the dens are also characteristic. Dual-energy CT (DECT) features include a dual-energy index (DEI) between 0.016-0.036.	
Radiographic osteoarthritis at hand/wrist[++]		
2nd or 3rd metacarpophalangeal joint osteoarthritis	Present if the Kellgren and Lawrence (K&L) grade is 2 or higher at the joint [30]	unchanged
Scapho-trapezium joint osteoarthritis	Presence of either joint space narrowing or osteophyte at the scapho-trapezium joint [31]	unchanged

Wrist osteoarthritis	Present if the K&L grade is 2 or higher at the radiocarpal joint [30]	unchanged

*DEI is calculated by the following equation applied to the region of interest:

$$\mathrm{DEI} = \frac{(attenuation\ low - attenuation\ high)}{(attenuation\ low + \ attenuation\ high + 2000)}$$

[+] Ultrasound definitions for fibrocartilage, hyaline cartilage, and tendon are the previously validated OMERACT CPPD Ultrasound Subtask Force definitions [15-17]

**Crowned dens syndrome is characterized by a combination of clinical and imaging features. This definition pertains to the imaging features only.

[++] Radiographic osteoarthritis at these joints has been associated with CPPD [27-29]

Accepted Article